

© Springer-Verlag 2011

El Hadad, Amir A., et al. Preparation of sol-gel hybrid materials from gamma-methacryloxypropyltrimethoxysilane and tetramethyl orthosilicate: study of the hydrolysis and condensation reactions. *Colloid and Polymer Science*, 2011, 289(17-18), 1875-1883.

<http://dx.doi.org/10.1016/j.elecom.2011.11.011>



**Preparation of Sol-Gel Hybrid Materials from
 γ -Methacryloxypropyltrimethoxysilane and Tetramethyl
 Orthosilicate:
 Study of the Hydrolysis and Condensation Reactions**

Journal:	<i>Colloid and Polymer Science</i>
Manuscript ID:	CPS-2011-0366
Manuscript Type:	Original Contribution
Date Submitted by the Author:	10-Aug-2011
Complete List of Authors:	El hadad, Amir; Centro Nacional de Investigaciones Metalurgicas (CSIC) Carbonell, Diogenes; Universidad Carlos III de Madrid, Departamento de Ciencia e Ingeniería de Materiales e Ingeniería Química Barranco, Violeta; Instituto de Ciencia de Materiales de Madrid (CSIC) Jiménez-Morales, Antonia; Universidad Carlos III de Madrid, Departamento de Ciencia e Ingeniería de Materiales e Ingeniería Química Casal, Blanca; Centro Nacional de Investigaciones Metalurgicas (CSIC) Galvan, Juan; Centro Nacional de Investigaciones Metalurgicas (CSIC)
Keywords:	sol-gel, silica, organic-inorganic materials, organopolysiloxane precursors, Si-29 NMR , C-13 NMR, FTIR, structural characterization

1
2
3
4
5
6
7
8
9
10
11
12
13
14
15
16
17
18
19
20
21
22
23
24
25
26
27
28
29
30
31
32
33
34
35
36
37
38
39
40
41
42
43
44
45
46
47
48
49
50
51
52
53
54
55
56
57
58
59
60

**Preparation of Sol-Gel Hybrid Materials from
 γ -Methacryloxypropyltrimethoxysilane and Tetramethyl Orthosilicate:
Study of the Hydrolysis and Condensation Reactions**

A. A. El hadad¹, D. Carbonell², V. Barranco³, A. Jiménez-Morales²,
B. Casal¹, J.C. Galván¹

¹Centro Nacional de Investigaciones Metalúrgicas (CSIC), Madrid, Spain,

²Universidad Carlos III de Madrid. Departamento de Ciencia e Ingeniería de Materiales e Ingeniería
Química. (Madrid), Spain.

³Instituto de Ciencia de Materiales de Madrid (CSIC), Madrid, Spain.

e-mails: amirelhada@cenim.csic.es, jcgalvan@cenim.csic.es

Abstract. Organic-inorganic hybrid materials suitable for the development of sol-gel coatings for metallic surfaces were prepared by hydrolysis and condensation of γ -methacryloxypropyltrimethoxysilane (MAPTMS) and tetramethyl orthosilicate (TMOS). The hydrolysis of MAPTMS/TMOS was carried out in an ethanol/water solution. The prehydrolysis stage of MAPTMS/TMOS system was monitored by Fourier Transformer Infrared Spectroscopy (FTIR) and liquid-state ²⁹Si and ¹³C Nuclear Magnetic Resonance (²⁹Si and ¹³C NMR). FTIR analysis indicated that the hydrolysis of MAPTMS/TMOS was accomplished as far as the (Si-OMe) band corresponds to unhydrolyzed silane disappeared. The concentration of the alkoxy groups and the extent of self-condensation of mono-, di-, and tri-substituted siloxanes (T species) in the sol were estimated by using liquid-state ²⁹Si NMR spectroscopy. The hydrolysis of the prepared sol was also evaluated by liquid state ¹³C NMR spectroscopy. The results indicated that under the adopted synthesis strategy conditions, the hydrolysis process require four hours to be completed.

Keywords: sol-gel; silica; organic-inorganic materials; organopolysiloxane precursors; Si-29 and C-13 NMR; FTIR; structural characterization.

INTRODUCTION

The interest in developing novel organic-inorganic hybrid coatings in recent years is due to the unique properties derived from combining inorganic and organic components into a single system [1-7]. Inorganic and organic-inorganic sol-gel materials have many applications in diverse fields such optics, electronics, ionics, mechanics, energy, environment and biology [8,9], separation, catalysis and sensing

1
2
3
4
5
6
7
8 [10-15], electrochemistry [16-24], functional smart materials and corrosion protection coatings
9
10 [8,9,25,26] or biomaterials and biomedical applications [9,27-30]. The sol-gel route, originally directed
11
12 towards the synthesis of purely inorganic materials, is increasingly being extended to the preparation of
13
14 organic-inorganic hybrid materials. The organic-inorganic hybrids combine the desirable properties of
15
16 organic polymers (toughness, elasticity) with those of inorganic solids (hardness, chemical resistance).
17
18 The sol-gel method as a materials processing technique has attracted intense and growing interest of the
19
20 researchers because of its advantages over the other traditional preparation methods. This route enables
21
22 the obtaining of high reactivity, better purity, avoidance of corrosive by products, improved control of
23
24 the product structure and provides an easy, cost-effective and excellent way to incorporate inorganic
25
26 compounds into an organic one [31-33]. The organic-inorganic hybrid materials can be easily prepared at
27
28 room temperature by hydrolysis and condensation of metal alkoxides of the type $M(OR)_n$, where M is Si,
29
30 Ti, Al, Sn, Zr, etc. This method comprises a chemical synthesis of materials having an oxide backbone
31
32 and an additional organic component as a network former. Starting from hydrolyzable molecular
33
34 compounds, such as alkoxy compounds of silicon, for instance tetramethyl orthosilicate (TMOS), the
35
36 hydrolysis and condensation is induced by addition of water and a catalyst giving to the formation of an
37
38 inorganic silica network. The organic silane precursor, for instance γ -
39
40 methacryloxypropyltrimethoxysilane (MAPTMS), contains organic groups which act as network
41
42 modifiers. Due to the presence of these modifiers, the final silicon network gains different properties (e.g.
43
44 hydrophobicity, flexibility) depending on the nature of the organic group used [34]. The hydrolyzed Si-
45
46 OH silanol groups are able to react with hydroxyl groups present on inorganic or metal surfaces, to form
47
48 hydrogen bonds [35,36], followed by condensation to form oxane bonds [37,38]. Figure 1 shows a
49
50 simplify view of the cascade reactions of hydrolytic deposition of silanes on inorganic or metal surfaces.

51
52
53
54 The excess Si-OH groups adsorbed on the surface can also condense among themselves to form Si-O-Si
55
56 siloxane films [39]. Sol-gel coatings based on siloxane bonded units can be prepared starting from an
57
58 organic-inorganic hybrid system. Thus the co-hydrolysis and polycondensation of the MAPTMS and
59
60 TMOS mixture produce a polymeric structure (Figure 2), exhibiting properties of chemical compatibility
and flexibility able to accommodate other species, as selected ionophores or corrosion inhibitors, without

1
2
3
4
5
6
7
8 showing phase segregation neither cracking processes. We have used these precursors for multifunctional
9
10 purposes, to develop electrode-membranes [40,41], ion selective sensors [42,43] and self-repairing
11
12 coatings for delaying the corrosion advance in metals [44].
13

14
15 The aim of the current paper has been to study the structural changes which take place during the
16
17 hydrolysis and condensation processes of a MAPTMS/TMOS solution after the addition of water and
18
19 ethanol. FTIR and liquid-state ^{29}Si and ^{13}C NMR have been applied for this purpose.
20
21

22 **MATERIALS AND METHODS**

23 **Sol preparation**

24
25 As described in detail elsewhere [42-44], sols were prepared starting from a mixture of 4 mol of γ -
26
27 methacryloxypropyltrimethoxysilane (MAPTMS, Aldrich) and 1 mol of tetramethoxysilane (TMOS,
28
29 Fluka). Ethanol ($\text{C}_2\text{H}_5\text{OH}$, 99.8%) and water were added with the molar ratio silane/water/methanol of
30
31 1/3/3. The resulting sol solution was completely transparent and without phase separation.
32
33
34

35 **Fourier Transforms Infrared Spectrometer (FTIR).**

36
37 The prepared sol samples were analyzed by FTIR spectral analysis. Each sample was prepared by mixing
38
39 about 0.5 ml of sol with 200 mg of CSI, which was subsequently pressed into pellet in an evacuated die.
40
41 All the spectra were measured by using a Nicolet Magna 550 infrared spectrometer at room temperature,
42
43 which covers the wavenumber range of $4000\text{-}400\text{ cm}^{-1}$.
44
45
46
47

48 **Liquid-State Nuclear Magnetic Resonance (NMR).**

49
50 ^{29}Si and ^{13}C NMR spectra of the liquid samples were recorded at 79.49 and 100.62 MHz respectively, in a
51
52 Bruker AVANCE-400 spectrometer. The external magnetic field was 9.4 Tesla. The single pulse NMR
53
54 spectra were obtained after excitations with a $\pi/2$ pulse length of $6\mu\text{s}$, for ^{29}Si and intervals between
55
56 successive accumulations (recycle delay) of 5s for each type of signal. NMR spectra were registered for
57
58 ^{13}C with a $\pi/2$ pulse length of $5\mu\text{s}$ and a recycle delay of 10s. The number of scans was 1600 in the case
59
60 of ^{29}Si and 128 for ^{13}C . The ^{29}Si and ^{13}C chemical shift values are given relative to $\text{Si}(\text{CH}_3)_4$. The

1
2
3
4
5
6
7
8 deconvolutions of the NMR spectra were carried out with the WINFIT program so that the different
9 components, and their contributions, could be determined.
10

11 12 **RESULTS AND DISCUSSION**

13
14
15 The reaction between silanes species in liquid media occurs, in general, by sol-gel process in which
16 hydrolysis and condensation of the silane groups take place. In particular by mixing the two precursors
17 (MAPTMS/TMOS) with H₂O/ethanol at ambient temperature, the hydrolysis taking place in the solution
18 must be considered [45].
19
20
21
22
23

24 In this sense, FTIR is a rapid, nondestructive and sensitive analytical method for identifying functional
25 groups present. The FTIR spectrum of the MAPTMS/TMOS upon mixing with EtOH/H₂O solvent system
26 can be seen in Figure 3. The corresponding band assignments are present in Table 1. The absorption bands
27 around 2950 and 2840 cm⁻¹ are attributed to stretching vibrations of C-H bonds in alkyl and methoxy
28 groups, respectively [46]. The band close to 1720 cm⁻¹ is associated to the stretching vibrations of C=O
29 carbonyl groups of MAPTMS, while that one at 1640 cm⁻¹ is attributed to C=C groups of the
30 methacrylate groups from the MAPTMS precursor [46-48].
31
32
33
34
35
36
37
38
39

40 The bands at 1450 and 1150 cm⁻¹ are attributed to deformation vibrations of C-H in CH₂ and CH₃ bonds
41 [49,50]. The asymmetric and symmetric stretching vibrations of C-O of C-O-C bonds are attributed to
42 bands at 1320 and 1300 cm⁻¹, respectively [49]. Finally, the bands at 941 and 822 cm⁻¹ are assigned to the
43 C=C vibrations of the C=C-C=O group, while that assigned to C-C-O skeleton vibration for pure ethanol
44 appear at 1090 cm⁻¹ [50]. All those bands (except the one at 2840 cm⁻¹) are related with the non-
45 hydrolysable part of the MAPTMS-TMOS mixture, and should appear in the FTIR spectra carried out
46 after the hydrolysis process.
47
48
49
50
51
52
53

54 The band at 1080 cm⁻¹ is attributed to stretching vibrations of Si-O-C bonds. Other authors have also
55 made the same attribution in different silanes [51,52]. This band is the one that expected to be broken
56 during the hydrolysis process. Presence of the very little bands assigned to Si-O-Si bonds at 980 cm⁻¹
57
58
59
60

1
2
3
4
5
6
7
8 indicates that certain condensation of the silane chains has taken place immediately upon mixing [53].
9
10 These bands prove the existence of condensation phenomena together with the hydrolysis one.

11
12 The FTIR spectra of the MAPTMS/TMOS aqueous mixture are shown in Figure 4, for hydrolysis time
13 varying from 15 minutes up to 3.5 h. In these spectra it is clearly observed that the FTIR spectrum of 3.5
14 h spectrum is very similar to that after 1 minute of mixing (Figure 3), which would indicate the
15 incomplete hydrolysis of the mixture.
16
17
18
19

20
21 As the hydrolysis time increases, 4 hours of hydrolysis, the spectra change substantially (Figure 5A). The
22 band at 2841 cm^{-1} , associated to the methoxy group, which appeared upon mixing (Figure 3), disappears
23 for hydrolysis times of four hours (Figure 5A). This allows establishing the beginning of optimal
24 hydrolysis conditions at about 4 hours. The same happens with the asymmetric stretching vibration of the
25 Si-O-C, which was appeared at 1080 cm^{-1} (Figure 3). This bond is the one that must be broken during the
26 hydrolysis, and its absence in Figure 5A implies the end of the hydrolysis process [53]. This band
27 disappeared and replaced by two bands corresponding to Si-O-Si results from the condensation process.
28 Disappearance of the band of Si-O-CH₃ groups at 2840 cm^{-1} were also evidenced together with the
29 increase of a broad band at 3420 cm^{-1} , assigned to OH groups from SiOH formed through hydrolysis
30 [53]. Figure 5 shows that for the hydrolysis time of 8 up to 24 hours, the slight broadening of Si-O-Si
31 bands results from a highly cross linked network mainly consisting of linear polysiloxanes with a mixture
32 of small and long chains.
33
34
35
36
37
38
39
40
41
42
43
44
45

46 The NMR nuclear magnetic resonance is a useful tool to study the silane hydrolysis; the NMR relaxation
47 time measurements are sensitive to short-range interactions and can be used to estimate the scale of
48 miscibility of an organic-inorganic hybrid [54]. This is due to the good resolution and quantitative
49 assignment of the NMR peaks of silane molecules in comparison with the FTIR analysis [55].
50
51
52
53
54
55

56 Liquid-state ^{29}Si and ^{13}C NMR have been applied to study the hydrolysis mechanism of the
57 MAPTMS/TMOS mixture in EtOH-H₂O solution. In the ^{29}Si NMR spectroscopy, the chemical shift of
58 silicon is determined by the chemical nature of their neighbours, namely T, and Q structures [56].
59
60

1
2
3
4
5
6
7
8 A Q species is one in which the Si atom is capable of producing four siloxane bonds, results from TMOS
9 precursor, whereas a T can only achieve three siloxane bonds and results from MAPTMS [31]. According
10 to the nomenclature, four T signals of different nature can be present (T^n , where $n=0; 1; 2; \text{ or } 3$,
11 respectively) [32]. Figure 6 shows a schematic representation of T^n silane structures. T^0 appears in a
12 spectral range from -37 to -39 ppm which is assigned to $\text{RSi}(\text{OCH}_3)_3$ unhydrolyzed species from
13 MAPTMS. T^1 occurs in the range defined between -46 to -48 ppm, assigned to condensed silicon units
14 bearing only one bridging oxygen atom (Si-O-Si), T^2 is defined in the spectral range defined between -53
15 to -57 ppm which is assigned to doubly condensed silicon centres (two bridging oxygen atoms), and T^3 is
16 defined into the -61 to -66 ppm range, fully condensed silicon units (three bridging oxygen atom) as
17 sketched in the Figure 6 [56].
18
19
20
21
22
23
24
25
26
27
28

29 The ^{29}Si spectra of MAPTMS /TMOS in EtOH- H_2O solution are shown in Figure 7. Upon mixing of the
30 two precursors (Figure 7A), the $\text{RSi}(\text{OCH}_3)_3$ species from non-hydrolyzed MAPTMS (T^0 units) give a
31 well detectable singlet signal at -42 ppm. The appearance of mono-, di-, and tri-substituted siloxanes T
32 species (T^1 units at -50 ppm, T^2 units at -59 ppm, and T^3 units between -68 and -71 ppm) is a result of the
33 self condensation. These observations are in agreement with the FTIR results which showed the presence
34 of condensed siloxane species at 980 cm^{-1} upon mixing of the two precursors, indicated by presence of
35 the Si-O-Si band (Figure 3). The $\text{Si}(\text{OCH}_3)_4$ unhydrolyzed species from TMOS were not detected in the
36 ^{29}Si spectra upon mixing of the two precursors with H_2O /ethanol and this because TMOS was used in
37 little amount and so has been hydrolyzed upon mixing.
38
39
40
41
42
43
44
45
46
47

48 After 1 hour of the reactive mixing, both the T^1 at 49.81 ppm and T^2 at 58 became clear and dominate the
49 entire spectrum which indicates the progress of the hydrolysis process (Figure 7B). Also the T^3 of
50 hydrolyzed MAPTMS and Q^2 and Q^3 of hydrolyzed TMOS appear as very small signals at 67.55, 91.78
51 and 101.66 ppm, respectively.
52
53
54
55
56

57 After 2 hours of hydrolysis and up to 3 hours (Figures 7C and 7D), there is not a significant change
58 between these spectra and that of after 1 hour and the concentrations of condensed T^2 and T^1 species units
59 remain constant (Figure 7B).
60

1
2
3
4
5
6
7
8
9 After 4 hours of hydrolysis, the T species in the form of T¹, T² and T³ at -50, -58 and -68 ppm dominate
10 the entire spectrum (Figure 7E). These results shed light upon two important observations which indicate
11 that 4 hours were enough for the hydrolysis of the of MAPTMS/TMOS mixture, in a similar way as the
12 FTIR spectra has indicated. It can observe:
13
14
15

- 16 • The non existence of unhydrolyzed TMOS, (Si (OCH₃)₄), as it hydrolyzed very rapidly.
- 17 • The disappearance of the signal T⁰ corresponding to the initial unhydrolyzed MAPTMS (Figure
18 7A).
- 19 • The appearance of the signal T³, which correspond fully to condensed silicon units with three
20 siloxane bonds (three bridging oxygen atom) dominated all the spectrum of 4 hours.
21
22
23
24
25
26
27

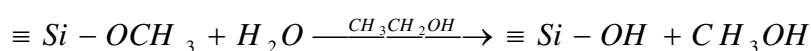
28
29 The ²⁹Si NMR spectra provide the proportions of Tⁿ species (n=1; 2; or 3), where T represents a Si atom
30 oxygen bridged to another Si atoms. These allowed the quantification of the crosslinking degree within
31 the silicate network. The T¹, T² and T³ units arose from the self-condensation reactions only. The T¹ units
32 represented dimers or chain ends. The T² were associated with the linear siloxane sequences, and the T³
33 units witnessed about the appearance of three-dimensional siloxane networks. In fact, the non-reacted
34 silane molecules (T⁰ units) from MAPTMS gave a well detectable singlet signal at -42 ppm (Figure 7A).
35 This singlet disappeared from the spectrum after 1 hours of reactive mixing, indicating beginning of
36 hydrolysis reaction.
37
38
39
40
41
42
43
44
45

46 As it was expected from the FTIR results, the maximum of self-condensed products was observed after 4
47 hours of reaction. The proportions of the T species in each hybrid system quoted in Table 2 were obtained
48 from deconvolution of the ²⁹Si NMR spectra with the WINFIT software. The spectra were deconvolved
49 into individual Gaussian line shapes, thus allowing a quantitative analysis of the spectra based on the peak
50 areas of each species. From Figure 8, it can be seen that after 4 hours of hydrolysis the amount of T³
51 silicon content increased while that of T² and T³ silicon content decreased in the matrix of the Si-O-Si
52 structure. That the hydrolysis was accompanied by a condensation reaction among the silanol groups to
53 give oligomeric structures.
54
55
56
57
58
59
60

The ^{13}C NMR spectra of MAPTMS/TMOS in EtOH-H₂O is shown in Figures 9 and 10. This mixture was hydrolyzed for 4 hours in EtOH-H₂O solution. In comparison with the ^{29}Si NMR spectra, the patterns of the ^{13}C NMR peak positions are significantly exhibiting multiple peaks. This suggests that there are several chemical compounds within the hybrid systems containing carbon-bonding structures. Peaks assignments for carbon-bonding types which can be attributed to the MAPTMS and TMOS precursors are given in Table 3. The peaks from TMOS and MAPTMS in the ^{13}C NMR spectra are in good agreement with earlier reports [57]. The hydrolysis of the MAPTMS/TMOS system was followed by the evolution of the peaks corresponding to the methyl groups attached to the silane and those liberated during the hydrolysis (CH₃-OH and CH₃-CH₂-OH).

Upon mixing of the two silane precursors with EtOH-H₂O solution, the peaks at 17.45 and 57.29 ppm are from ethoxy groups of ethanol and to CH₃-C of MAPTMS [58] (Figures 9A and 10A). The peaks at 48.97 are ascribed to unhydrolyzed CH₃-O-Si units of MAPTMS and TMOS. The peak at 67.10 ppm is attributable to CH₂-CH₂-O units of MAPTMS while that appear at 22.47 ppm are due to CH₂-CH₂-Si units of the same precursor. Finally, the peak at 9.18 ppm are attributed to Si-C of MAPTMS.

Up to 2 hour of reaction, no changes can be detected (Figures 9B-9C and Figures 10B-10C). Thus the spectrum exhibits the same peaks corresponding to the carbon within the hybrid systems containing carbon-bonding structures. After 3 hours of hydrolysis, the spectrum exhibit significant changes (Figures 9D and 10D). The peak that appear at 49 ppm corresponds to the release of methanol as a result of beginning of condensation process. The emergence of this peak indicates the hydrolysis of the methoxy group in (H₃C-O-Si) of both precursors. The hydrolysis of methoxy groups caused by water in ethanol, contributed to the yielding of methanol as a reaction product that it is seen in the liquid-state ^{13}C NMR spectra [59]:



At the same time, during the hydrolysis of TMOS in ethanol, methoxy groups of TMOS are exchanged for alkoxy groups. This reaction is an equilibrium reaction. Almost all of methoxy groups are exchanged for ethoxy groups. This give a well developed band that newly emerged at 7.62 and 57.26 ppm in the

1
2
3
4
5
6
7
8 spectrum of three hours hydrolysis (Figures 9D and 10D), corresponding to Si-O-CH₂-CH₃ units and
9 methanol is released into the solution following the next reaction.
10

11
12
13 After 4 hours of hydrolysis it takes place, the disappearance of the methoxy groups of the initial silanes
14 at 48.97 ppm and the concomitant formation of free methanol, as indicated by the peak growing at 49
15 ppm of hydrolyzed mixture [60] (Figure 10E). Thus the the disappearance of the resonances assigned to
16 the CH₃-O-Si group is accompanied by the increase of the CH₃-OH signal. All these facts can confirm
17 that four hours are enough for the hydrolysis reactions to be completed. These results indicated that the
18 hydrolyzable Si-O-CH₃ groups of both precursors were hydrolyzed and forming silanol groups that could
19 derive in Si-O-Si bonds due to subsequent condensation. This agrees well with the results obtained from
20 ²⁹Si NMR, that showed that the hydrolysis was accompanied by a condensation reaction among the
21 silanol groups to give oligomeric structures. The evidence of the presence of such structures was provided
22 by the broadening of the different peaks in the ¹³C NMR spectra.
23
24
25
26
27
28
29
30
31
32
33

34 35 CONCLUSIONS

36
37 The sol-gel reaction of the MAPTMS/TMOS system in EtOH/H₂O solution was studied by FTIR and
38 NMR. The aim of the study was to optimize the pre-hydrolysis times of both silanes and consequently
39 their use as precursors for hybrid materials. The early step of the condensation process was studied by
40 collecting ²⁹Si NMR spectra and the quantitative analysis of the condensed species was calculated in
41 terms of T¹, T² and T³ silicon units. It could be concluded that the hydrolysis of the two silane precursors
42 under the adopted synthesis strategy conditions is completed after approximately, four hours at room
43 temperature. The quantitative analysis of the NMR indicates that presence of self-condensation species
44 after mixing of the two precursors which react between them as the time proceeds results in progress of
45 the hydrolysis process. the hydrolysis was accompanied by a condensation reaction among the silanol
46 groups to give oligomeric structures.
47
48
49
50
51
52
53
54
55
56
57
58
59
60

ACKNOWLEDGEMENTS

This work has been supported by the Ministry of Science and Innovation of Spain (Projects MAT2006-04486 and MAT2009-13530) and the Regional Community of Madrid (Project 2009/MAT-1585). A.A. El hadad acknowledges a pre-doctoral contract JAE financed by CSIC and; V.B. acknowledges a Ramon y Cajal researcher contract financed by CSIC-MICINN.

REFERENCES

1. C.J. Brinker, C.W. Scherer Editors, in "Sol-Gel Science: The Physics and Chemistry of Sol-Gel Processing", Academic Press Inc, Boston, San Diego, New York (1990).
2. B.M. Novak, *Adv. Mater.*, **5**, 422 (1993).
3. C. Sanchez, F. Ribot, *New. J. Chem.*, **18**, 1007 (1994).
4. J.Y. Wen, G.L. Wilkes, *Chem. Mater.*, **8**, 1667 (1996).
5. A. Stein, B.J. Melde, R.C. Schroden, *Adv. Mater.*, **12**, 1403(2000).
6. P. Gomez-Romero, *Adv. Mater.*, **13**, 163 (2001).
7. C. Sanchez, G.J.D.A. Soler-Illia, F. Ribot, T. Lalot, C.R. Mayer, V. Cabuil, *Chem. Mater.*, **13**, 3061 (2001).
8. G. Schottner, *Chem.Mater.*, **13**, 3422 (2001).
9. C. Sanchez, B. Julian, P. Belleville, M. Popall, *J. Mater. Chem.*, **15**, 3559 (2005).
10. B. Casal, E. Ruiz-Hitzky, M. Crespín, D. Tinetti, J. C. Galván, *J. Chem. Soc., Faraday Trans. 1*, **85**, 4167 (1989).
11. E. Ruiz-Hitzky, P. Aranda, B. Casal, J.C. Galván, *Adv. Mater.*, **7**, 180 (1995)
12. J. Wang, J. Merino, P. Aranda, J.C. Galván, E. Ruiz-Hitzky, *J. Mater. Chem.*, **9**, 161 (1999).
13. E. Ruiz-Hitzky, P. Aranda, B. Casal, J.C. Galván, *Rev. Inorg. Chem.*, **21**, 125 (2001).
14. M.L. Rojas-Cervantes, B. Casal, P. Aranda, M. Savirón, J.C. Galván, E. Ruiz-Hitzky, *Colloid Polym. Sci.*, **279**, 990 (2001).
15. L. Nicole, C. Boissiere, D. Grosso, A. Quach, C. Sanchez, *J. Mater. Chem.*, **15** 35, 3598, (2005).
16. J.M. Amarilla, B. Casal, J.C. Galván, E. Ruiz-Hitzky, *Chem. Mater.*, **4**, 62 (1992).
17. J.C. Galván, P. Aranda, J.M. Amarilla, B. Casal, E. Ruiz-Hitzky, *J. Mater. Chem.*, **3**, 687 (1993).

- 1
- 2
- 3
- 4
- 5
- 6
- 7
- 8 18. P. Aranda, A. Jiménez-Morales, J.C. Galván, B. Casal, E. Ruiz-Hitzky, *J. Mater. Chem.*, **5**, 817 (1995) .
- 9
- 10 19. O. Lev, M. Tsionsky, L. Rabinovich, V. Glezer, S. Sampath, I. Pankratov, J. Gun, *Anal. Chem.*, **67** (1),
- 11 22A (1995).
- 12
- 13 20. O. Lev, Z. Wu, S. Bharathi, V. Glezer, A. Modestov, J. Gun, L. Rabinovich, S. Sampath, *Chem.*
- 14 *Mater.*, **9**, 2354 (1997).
- 15
- 16
- 17 21. B.Q. Wang, B. Li, Q. Deng, S.J. Dong, *Anal. Chem.*, **70**, 3170 (1998).
- 18
- 19 22. A. Walcarius, *Chem. Mater.*, **13**, 3351 (2001).
- 20
- 21 23. A. Walcarius, D. Mandler, J.A. Cox, M. Collinson, O. Lev, *J. Mater. Chem.*, **15**, 3663 (2005).
- 22
- 23 24. M. Popall, M. Andrei, B. Olsowski, *Electrochim. Acta*, **43**, 1155 (1998).
- 24
- 25 25. M.L. Zheludkevich, I.M. Salvado, M.G.S. Ferreira, *J. Mater. Chem.*, **15**, 5099 (2005).
- 26
- 27 26. V. Barranco, N. Carmona, J.C. Galván, M. Grobelny, L. Kwiatkowski, M.A. Villegas, *Prog. Org.*
- 28 *Coat.*, **68**, 347 (2010).
- 29
- 30 27. L.L. Hench, *J. Am. Ceram. Soc.*, **74**, 1487 (1991).
- 31
- 32 28. L.G. Griffith, G. Naughton, *Science*, **295** (5557) 1009 (2002).
- 33
- 34 29. T. Kokubo, H.M. Kim, M. Kawashita, *Biomaterials*, **24**, 2161 (2003).
- 35
- 36 30. R. Langer, D.A. Tirrell, *Nature*, **428** (6982), 487 (2004).
- 37
- 38 31. C.J. Brinker and C.W. Scherer, in "Sol-Gel Science: The Physics and Chemistry of Sol-Gel
- 39 Processing", Academic Press Inc., Boston, San Diego, New York, p. 97. (1990).
- 40
- 41 32. G. Philipp and H. Schmidt, *J. Non-Cryst. Solids*, **63**, 283 (1984).
- 42
- 43 33. H. Schmidt, *Mater. Res. Soc. Symp. Proc.*, **32**, 327 (1984).
- 44
- 45 34. Oun-H. Park, Young-Joo Eo, Yoon-Ki Choi and Byeong-Soo Bae. *J. Sol-Gel Sci. and Technol.*,
- 46 **16**, 235 (1999).
- 47
- 48 35. F.D. Osterholz, E.R. Pohl, *J. Adhesion Sci. Technol.*, **6**, 127 (1992).
- 49
- 50 36. F.D. Blum, W. Meesiri, H.J. Kang, J.E. Gambogi, *J. Adhesion Sci. Technol.*, **5**, 479 (1991).
- 51
- 52 37. B. Arkles, J. R. Steinmetz, J. Zazyczny, P. Mehta, *J. Adhesion Sci. Technol.*, **6**, 193 (1992).
- 53
- 54 38. P. Walker, in "Handbook of Adhesive Technology", Second Edition, Revised and Expanded, A.
- 55 Pizzi and K. L. Mittal Editors, Marcel Dekker Inc ., New York / Basel, pp. 205-221 (2003).
- 56
- 57 39. C.W. Chu, D.P. Kirby, P.D. Murphy, *J. Adhesion Sci. Technol.*, **7**, 417(1993).
- 58
- 59
- 60

- 1
- 2
- 3
- 4
- 5
- 6
- 7
- 8 40. A. Jiménez-Morales, J.C. Galván, P. Aranda, E. Ruiz-Hitzky, *Mater. Res. Soc. Symp. Proc.*, **519**,
- 9 211 (1998).
- 10
- 11 41. E. Ruiz-Hitzky, J. C. Galván, P. Aranda, A. Jiménez-Morales, Spanish Patent, P. 9900956, 1999.
- 12
- 13 42. A. Jimenez-Morales, J.C. Galvan, P. Aranda, *Electrochim. Acta*, **47 (13-14)**, 2281 (2002).
- 14
- 15 43. A. Jiménez-Morales, P. Aranda, J.C. Galván, *J. Mater. Process. Technol.*, **143-144**, 5 (2003).
- 16
- 17 44. M. Garcia-Heras, A. Jimenez-Morales, B. Casal, J.C. Galvan, S. Radzki, M.A. Villegas, *J. Alloy.*
- 18 *Compd.*, **380 (1-2)**, 219 (2004).
- 19
- 20
- 21 45. D.Wang, G.P. Bierwagen, *Prog. Org. Coat.*, **64**, 327 (2009).
- 22
- 23 46. M.A. Rodriguez, M.J. Liso, F. Rubio, J. Rubio, J.L. Oteo, *J. Mater. Sci.*, **34**, 3867 (1999).
- 24
- 25 47. J.P. Matinlinna, M. Ozcan, L.V.J. Lassila, P.K. Vallittu, *Dent. Mater.*, **20**, 804 (2004).
- 26
- 27 48. M. Abdelmouleha, S. Boufia, M.N. Belgacemb, A. Dufresne, *Compos. Sci. Technol.*, **67**,1627
- 28 (2007).
- 29
- 30
- 31 49. P. Innocenzi, G. Brusatin, *J. Non-Cryst. Solids*, **333**, 137 (2004).
- 32
- 33 50. A. Franquet, H. Terryn, J. Vereecken, *Appl. Surf. Sci.*, **211**, 259 (2003).
- 34
- 35 51. Z. Danqing, W.J. van Ooij, *J. Adhes. Sci. Technol.*, **16** (2002) 1235.
- 36
- 37 52. T. Gunji, Y. Makabe, N. Takamura, Y. Abe, *Appl. Organomet. Chem.*, **15**, 683 (2001).
- 38
- 39 53. Sunirmal Jana, Mi Ae Lim, In Chan Baek, Chang Hae Kim, Sang Il Seok, *Mater. Chem. Phys.*, **112**,
- 40 1008 (2008).
- 41
- 42 54. N. Nisiyama and K. Horie, *J. Appl. Polym. Sci.*, **34**,1619 (1987).
- 43
- 44 55. M.C.B. Salon, P.A. Bayle, M. Abdelmouleh, S. Boufic, M.N. Belgacem, *Colloid Surf. A-*
- 45 *Physicochem. Eng. Asp.*, **312**, 83 (2008).
- 46
- 47 56. R.H. Glaser, G.L. Wilkes, *Polym. Bull.*, **19**, 51(1988).
- 48
- 49 57. C.L. Chiang, C.C.M. Ma, *Polym. Degrad. Stab.*, **83**, 207 (2004).
- 50
- 51 58. Y.H. Han, A. Taylor, M.D. Mantle, K.M. Knowles, *J. Non-Crystalline Solids*, **353**, 313-320 (2007).
- 52
- 53 59. K. Miyatake, O. Ohama, Y. Kawahara, A. Urano, A. Kimura, *Sei Technical Review*, No. 65, 21-24
- 54 (2007).
- 55
- 56 60. M.C.B Salon, M. Abdelmouleh, S. Boufi, M.N. Belgacem, A. Gandini, *J. Colloid Interface Sci.* **289**,
- 57 249-261(2005).
- 58
- 59
- 60

61. LIST OF TABLES

Table 1. Assignment of the FTIR peaks shown in Figure 3.

Table 2. Relative proportions of T and Q species in the organic–inorganic hybrid materials from the liquid-state ^{29}Si NMR spectra in Figure 7.

Table 3. Peaks assignments of liquid-state ^{13}C NMR spectra of both MAPTMS and TMOS according to peaks detected in Figure 9.

LIST OF FIGURES

Figure 1. Reaction and bonding mechanism of alkoxy silanes.

Figure 2. Schematic representation of the polymerization reaction of the MAPTMS and TMOS mixture producing a 3D organic-inorganic hybrid network.

Figure 3. FTIR spectrum of the MAPTMS/TMOS mixture in EtOH-H₂O solvent system upon mixing.

Figure 4. FTIR spectra of the MAPTMS/TMOS mixture in EtOH/H₂O solvent system. Hydrolysis time up to three hours and a half.

Figure 5. FTIR spectra of MAPTMS/TMOS mixture in EtOH/H₂O solvent system. Hydrolysis time up to twenty four hours. (A) 4 hours (B) 8 hour. (C) 12 hours (D) 24 hours.

Figure 6. Schematic representation of Tⁿ silane structures; n=1,2, or 3.

Figure 7. Liquid-state ^{29}Si NMR spectra of MAPTMS/MOS mixture in EtOH-H₂O solvent system. (A) Upon mixing of MAPTMS and TMOS (B) After one hour. (C) after two hours (D) after three hours (E) after four hours

Figure 8. Relationship of the signals, for species T⁰, T¹, T² and T³ in the MAPTMS/TMOS hybrid.

Figure 9. Liquid-state ^{13}C NMR spectra (0-30 ppm range) of prehydrolyzed MAPTMS/TMOS mixture. (A) Upon mixing of MAPTMS and TMOS, (B) after 1 hour, (C) after 2 hours, (D) after 3 hours and, (E) after 4 hours.

Figure 10. Liquid-state ^{13}C NMR spectra (40-70 ppm range) of the prehydrolyzed MAPTMS/TMOS mixture. (A) Upon mixing of MAPTMS and TMOS, (B) after 1 hour, (C) after 2 hours, (D) after 3 hours and, (E) after 4 hours.

Table 1. Assignment of the FTIR peaks shown in Figure 3

Wavenumber (cm^{-1})	Assignment	References
2950	$\nu_{\text{as C-H}}(\text{CH}_3)$	[46]
2840	$\nu_{\text{s C-H}}(\text{O-CH}_3)$	[46]
1720	$\nu_{\text{s C=O}}$ (methacryloxy group)	[46-48]
1640	$\nu_{\text{C=C}}$ (methacryloxy group)	[46-48]
1450	δ_{CH_2} (Si-R organic group)	[49,50]
1320	$\nu_{\text{as C-O}}$ (C–O–C bonds)	[49]
1300	$\nu_{\text{s C-O}}$ (C–O–C bonds)	[49]
1080	$\nu_{\text{as Si-O}}$ (Si–O–CH ₃)	[51]
1187	ν_{as} (Si–O–Si)	[53]
1085	ν_{s} (Si–O–Si)	[53]
3100-3600	$\nu_{\text{O-H}}$ (Si–OH)	[53]

s: symmetric; as: asymmetric

Table 2. Relative proportions of T and Q species in the organic–inorganic hybrid materials from the liquid-state ^{29}Si NMR spectra in Figure 7

Time in M	Proportions ^a (%)						Relative ^b proportions (%)				Relative proportions ^c (%)		Ratio ^d (%)	
	T ⁰	T ¹	T ²	T ³	Q ²	Q ³	T ⁰	T ¹	T ²	T ³	Q ²	Q ³	T ⁿ	Q ⁿ
	1	47.66	10.87	9.64	31.83	0	0	47.66	10.87	9.64	31.83	-	-	1
60	-	40.28	38.48	11.08	3.21	6.95	-	44.83	42.83	12.34	31.5	68.5	89.8	10.2
120	-	41.38	36.80	7.83	6.52	7.47	-	48.11	42.78	9.11	46.6	53.4	86	14
180	-	50.41	35.35	4.45	4.2	5.59	-	55.88	39.18	4.93	42.90	57.1	90	10
240	-	9.91	35.56	54.53	-	-	-	9.91	35.56	54.53	-	-	1	-

^a Proportions (%): these were calculated by the deconvolution technique. Error value assumed is $\pm 1\%$.

^b Relative proportions (%): (each T species/total T species) · 100%.

^c Relative proportions (%): (each Q species/total Q species) · 100%.

^d Ratio (%): $T_i = \{\text{total T species}/(\text{T species} + \text{Q species})\} \cdot 100\%$, $Q_j = \{\text{total Q species}/(\text{T species} + \text{Q species})\} \cdot 100\%$.

Table 3. Peaks
state ^{13}C NMR spectra of
TMOS according to
9

MAPTMS (Aldrich)		TMOS (Aldrich)		Ethanol	
Nature of carbons	Ass.(ppm)	Nature of carbons	Ass.(ppm)	Nature of carbons	Ass.(ppm)
$\text{CH}_2\text{-}\underline{\text{C}}\text{H}_2\text{-O}$	67.10	$\underline{\text{C}}\text{H}_3\text{-O-Si}$	48.97	$\text{CH}_2\text{-OH}$	57.29
$\text{CH}_3\text{-O-Si}$	48.97			$\underline{\text{C}}\text{H}_3\text{-CH}_2$	17.45
$\text{CH}_2\text{-CH}_2\text{-Si}$	22.47				
$\underline{\text{C}}\text{H}_3\text{-C}$	17.45				
$\text{CH}_2\text{-Si}$	9.18				

assignments of liquid-
both MAPTMS and
peaks detected in Figure

1
2
3
4
5
6
7
8
9
10
11
12
13
14
15
16
17
18
19
20
21
22
23
24
25
26
27
28
29
30
31
32
33
34
35
36
37
38
39
40
41
42
43
44
45
46
47
48
49
50
51
52
53
54
55
56
57
58
59
60

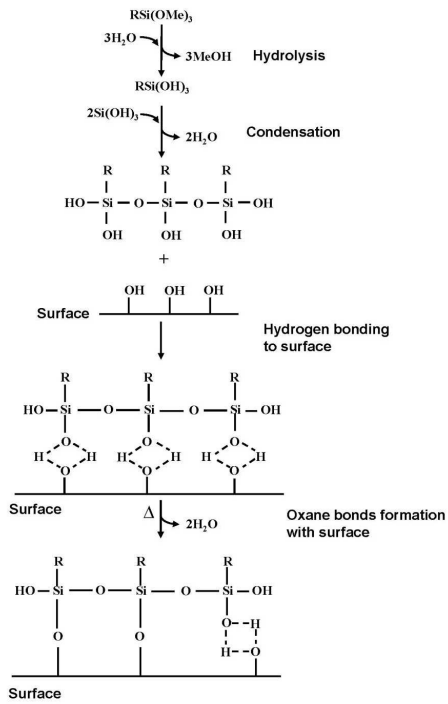


Figure 1. Reaction and bonding mechanism of alkoxy-silanes

1

210x297mm (200 x 200 DPI)

POLYMERIZATION:

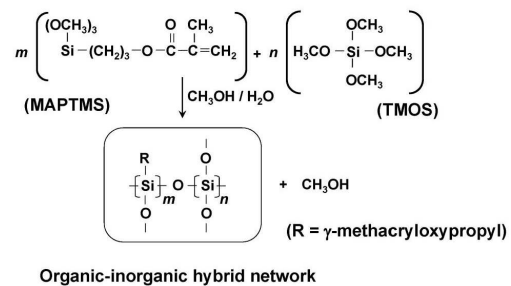


Figure 2. Schematic representation of the polymerization reaction of the MAPTMS and TMOS mixture producing a 3D organic-inorganic hybrid network

1
2
3
4
5
6
7
8
9
10
11
12
13
14
15
16
17
18
19
20
21
22
23
24
25
26
27
28
29
30
31
32
33
34
35
36
37
38
39
40
41
42
43
44
45
46
47
48
49
50
51
52
53
54
55
56
57
58
59
60

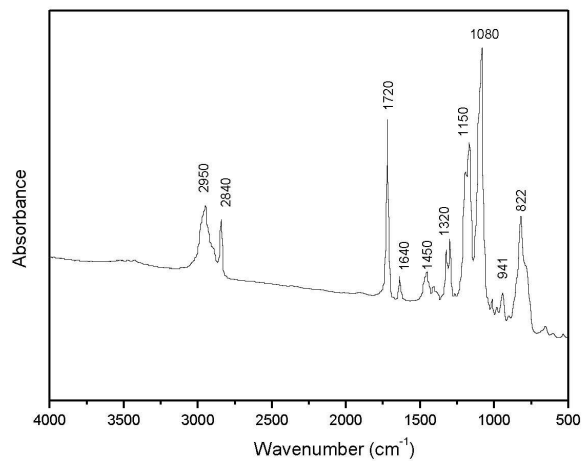


Figure 3. FTIR spectrum of the MAPTMS/TMOS mixture in EtOH-H₂O solvent system upon mixing

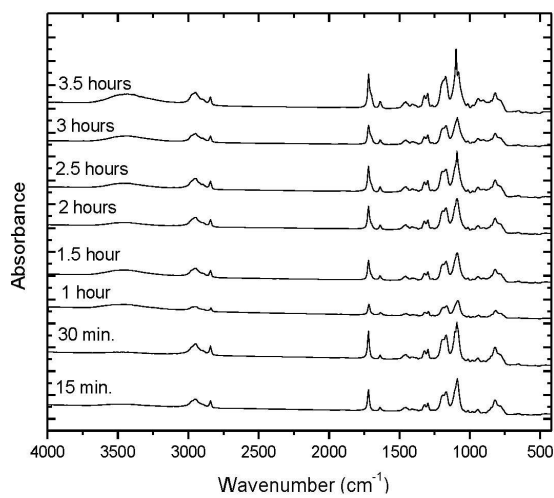


Figure 4. FTIR spectra of the MAPTMS/TMOS mixture in EtOH/H₂O solvent system. Hydrolysis time up to three hours and a half

1
2
3
4
5
6
7
8
9
10
11
12
13
14
15
16
17
18
19
20
21
22
23
24
25
26
27
28
29
30
31
32
33
34
35
36
37
38
39
40
41
42
43
44
45
46
47
48
49
50
51
52
53
54
55
56
57
58
59
60

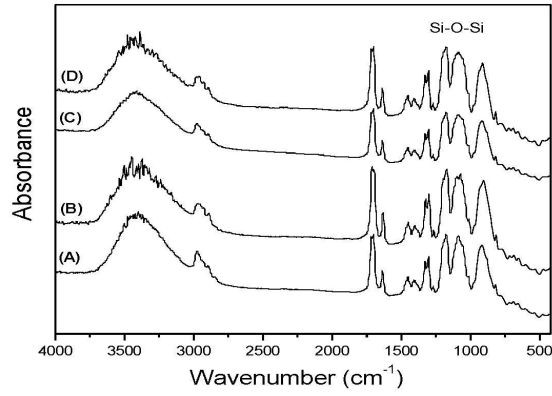


Figure 5. FTIR spectra of MAPTMS/TMOS mixture in EtOH/H₂O solvent system. Hydrolysis time up to twenty four hours. (A) 4 hours (B) 8 hour. (C) 12 hours (D) 24 hours

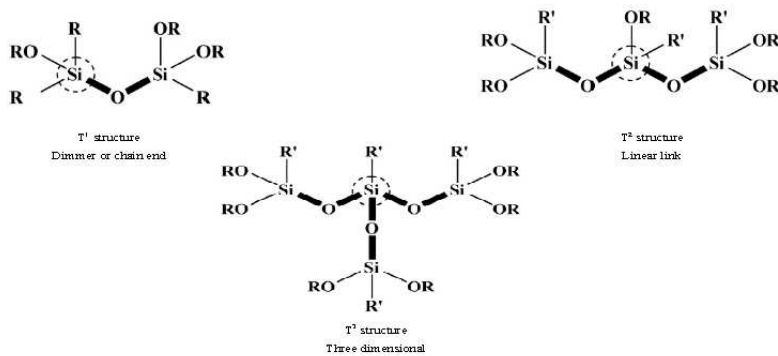


Figure 6. Schematic representation of Tⁿ silane structures (n=1, 2, or 3)

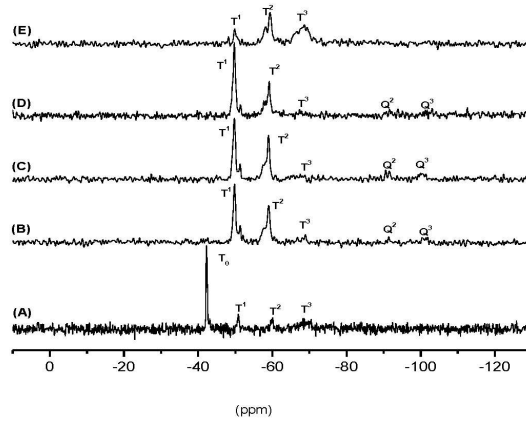


Figure 7. Liquid state ^{29}Si NMR spectra of MAPTMS/MOS mixture in EtOH-H₂O solvent system. (A) Upon mixing of MAPTMS and TMOS (B) After one hour. (C) after two hours (D) after three hours (E) after four hours

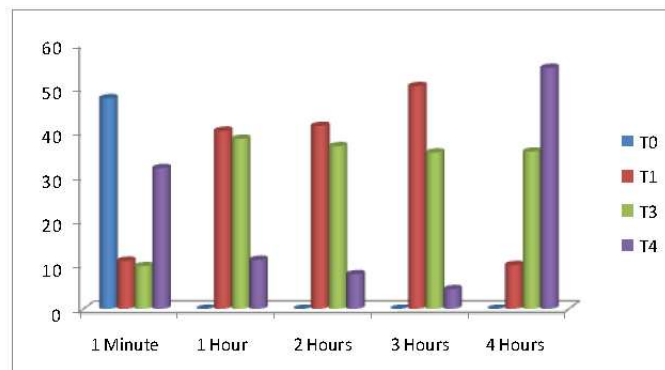


Figure 8. Relationship of the signals, for species T^0 , T^1 , T^2 and T^3 in the MAPTMS/TMOS hybrid

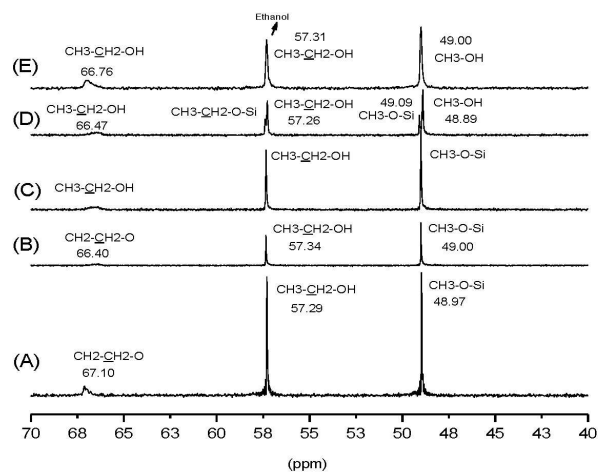


Figure 9. Liquid state ^{13}C NMR spectra (0-30 ppm range) of prehydrolyzed MAPTMS/TMOS mixture. (A) Upon mixing of MAPTMS and TMOS, (B) after 1 hour, (C) after 2 hours, (D) after 3 hours and, (E) after 4 hours

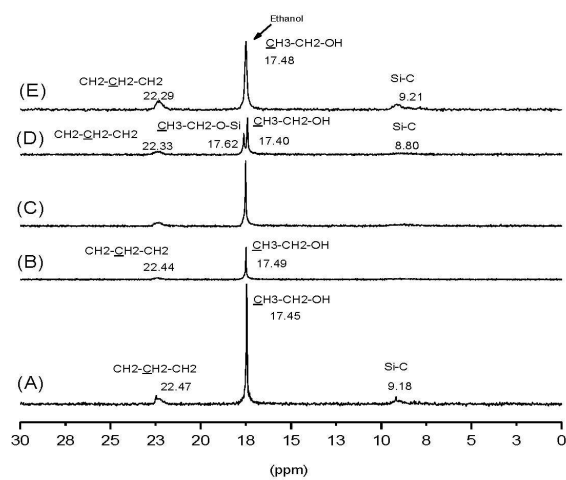


Figure 10. Liquid state ^{13}C NMR spectra (40–70 ppm range) of the prehydrolyzed MAPTMS/TMOS mixture. (A) Upon mixing of MAPTMS and TMOS, (B) after 1 hour, (C) after 2 hours, (D) after 3 hours and, (E) after 4 hours